ORIGINAL RESEARCH

Eupatilin inhibits glioma proliferation, migration, and invasion by arresting cell cycle at G1/S phase and disrupting the cytoskeletal structure

Xiaowei Fei[1,2]
Ji Wang[1]
Chen Chen[1]
Boyun Ding[1]
Xiaojun Fu[1]
Wenjing Chen[1]
Chongwu Wang[1]
Ruxiang Xu[1]

[1]Institute of Neurosurgery, Affiliated Bayi Brain Hospital, General Army Hospital, Beijing 10000, People's Republic of China; [2]Department of Physiology, Dalian Medical University, Dalian 116044, People's Republic of China

Purpose: Eupatilin is a pharmacologically active flavonoid extracted from Asteraceae argyi that has been identified as having antitumor effects. Gliomas are the most common intracranial malignant tumors and are associated with high mortality and a poor postoperative prognosis. There are few studies on the therapeutic effects of eupatilin on glioma. Therefore, we explored the efficacy and the underlying molecular mechanism of eupatilin on glioma.
Methods: The effect of eupatilin on cell proliferation and viability was detected using Cell Counting Kit-8 assays. Cell migration was analyzed with a scratch wound healing assay and invasion was analyzed using transwell assays.
Results: We found that eupatilin significantly inhibits the viability and proliferation of glioma cells by arresting the cell cycle at the G1/S phase. In addition, eupatilin disrupts the structure of the cytoskeleton and affects F-actin depolymerization via the "P-LIMK"/cofilin pathway, thereby inhibiting the migration of glioma. We also found that eupatilin inhibits the invasion of gliomas. The underlying mechanism may be related to the destruction of epithelial–mesenchymal transition, with eupatilin also affecting the RECK/matrix metalloproteinase pathway. However, we did not observe the proapoptotic effect of eupatilin on glioma, which is inconsistent with other studies. Finally, we observed a significant inhibitory effect of eupatilin on U87MG glioma in xenograft nude mice.
Conclusion: Eupatilin inhibits the viability and proliferation of glioma cells, attenuates the migration and invasion, and inhibits tumor growth in vivo, but does not promote apoptosis. Therefore, due to the poor clinical efficacy of drug treatment of glioma and high drug resistance, the emergence of eupatilin brings a new dawn for glioma patients.
Keywords: eupatilin, glioma, proliferation, cell cycle, migration, invasion

Introduction

Gliomas are the most common primary brain tumors induced by the brain and spinal glial lesions. The incidence of glioblastoma is about 3.2/100000.[1] The symptoms and signs of gliomas mainly depend on their location and the affected brain functions. Gliomas can cause headache, nausea, vomiting, epilepsy, blurred vision, and other symptoms due to its "mass effect" in space.[2] In addition, due to its influence on the function of local brain tissue, the patient can also exhibit other symptoms. For example, optic nerve gliomas lead to loss of vision in patients,[3] spinal cord gliomas cause pain, numbness, and weakness in limbs;[4] central gliomas cause movement and sensory disturbances in patients;[2] and gliomas affecting the

Correspondence: Chongwu Wang;
Ruxiang Xu
Institute of Neurosurgery, Affiliated Bayi Brain Hospital, General Army Hospital, No. 5, Nanmencang, Dongcheng District, Beijing 10000, People's Republic of China
Tel +861 520 142 8092;
+861 884 267 9884
Email darklordwcw@163.com;
524727684@qq.com

brain region involved in language cause difficulty in language expression and understanding.[5] The severity of symptoms caused by gliomas differs due to their differing degrees of malignancy.

The treatment of brain tumors mainly includes surgical resection, radiation therapy, and systemic drug therapy. For malignant brain tumors, a combination of treatments is often employed. Surgical resection is the main treatment of brain tumors, especially benign tumors. Radiation therapy is often used in patients who have no residual resection or surgical resection and can also be used in patients who are unlikely to undergo surgery.[6,7] In recent years, drug therapy primarily involves the monoclonal antibody bevacizumab. Temozolomide is effective in the treatment of gliomas, but long-term studies have shown resistance. Traditional Chinese medicine has always been a medical secret. With the development of science and technology, the medicinal ingredients in traditional Chinese medicine have gradually surfaced and have become an important means to inhibit tumor growth. Chen and colleagues found that plumbagin inhibits invasion and migration of glioma cells by downregulating matrix metalloproteinase (MMP)-2/9 expression and inhibiting PI3K/Akt signaling pathway.[8] A study reported by Lin and colleagues revealed that berberine enhances inhibition of glioma tumor cell invasiveness and migration mediated by arsenic trioxide.[9] Curcumin regulates the cell cycle progression of human glioma cell SHG44 in vitro, inducing the differential expression of Bcl-2 and Caspase 8, and significantly inhibits tumor cell proliferation and promotes apoptosis.

Eupatilin is a pharmacologically active flavonoid extracted from Asteraceae argyi. Eupatilin has been shown to have anti-inflammatory abilities and is used for mucosal protection. It has an antioxidant effect on gastric mucosal damage and can enhance the regeneration of damaged mucosa. Therefore, it is widely used to treat gastritis and peptic ulcers.[10] Eupatilin was identified as having antitumor effects; eupatilin suppresses angiogenesis in gastric cancer cells by altering the expression of signal transduction molecules and vascular endothelial growth factor (VEGF), and by activation of signal transducers and activator of transcription 3.[11] Eupatilin is used as an anti-metastatic and chemo-preventive agent for human gastric cancer.[12] Eupatilin inhibits the growth of human endometrial cancer cells by upregulating p21 to arrest the cell cycle in the G2/M phase.[13] Eupatilin also inhibits angiogenesis-mediated human hepatocyte metastasis by decreasing expression of VEGF and MMP-2.[14]

However, few studies have reported the effects of eupatilin on gliomas. Based on eupatilin effects on different tumors, we explored its effect and underlying mechanisms on glioma through in vitro cell experiments and in vivo BALB/c nude mice.

Materials and methods
Cell culture

Human malignant glioma (glioblastoma) cell lines U251MG, U118, T98G, and U87MG were provided by the Seventh Medical Center of the Chinese People's Liberation Army General Hospital. Cell line usage was approved by the General Army Hospital institutional review board or ethics committee. The cell lines were cultured in DMEM media supplemented with 10% serum and incubated at 37°C with 5% CO_2. FBS was purchased from Gibco (Cat. No. 10099141). DMEM was purchased from Corning Co., Ltd. (Cat. No. SJ.CELLGRO.10-013-CVR). Antibiotic was purchased from Sigma Aldrich (Cat. No. V900929).

Reagents

Cell Counting Kit-8 (CCK-8) was purchased from Dojindo Chemical Technology Co., Ltd., Shanghai, China (Cat. No. CK04). Eupatilin was purchased from Chengdu Purifa Technology Development Co., Ltd., China (Cat. No. BP0576) and was dissolved in DMSO. Matrigel was purchased from Corning Co., Ltd. (Cat. No. 356234). FITC Annexin V Apoptosis Detection Kit with PI was purchased from BioLegend (Cat. No. 640914). Cycle detection kit (Cat. No. C1052) and DiI (Cat. No. C1036) were purchased from Beyotime. Deoxyribonuclease I, Alexa Fluor TM 594 conjugate was purchased from Thermo Fisher Scientific (Cat. No. D12372). Phalloidin-iFluor 488 was purchased from Abcam (Cat. No. ab176753). Anti-Cofilin (Cat. No. ab124979), Anti-Profilin (Cat. No. ab124904), Anti-Calreticulin (Cat. No. ab92516), Anti-Ki67 (Cat. No. ab15580), and Anti-GM130 (Cat. No. ab52649) were purchased from Abcam. Anti-Cyclin A2 (Cat. No. 4656), Anti-Cyclin E2 (Cat. No. 4132), Anti-p21 Waf1/Cip1 (Cat. No. 2947), Anti-Phospho-Histone H3 (Ser10) (Cat. No. 3377), Anti-Phospho-Wee1 (Ser642) (Cat. No. 4910), Anti-Myt1 (Cat. No. 4282), Anti-Phospho-cdc2 (Tyr15) (Cat. No. 4539), Anti-Cyclin B1 (Cat. No. 12231), Anti-Phospho-p70 S6 Kinase (Thr421/Ser424) (Cat. No. 9204), Anti-Phospho-p73 (Tyr99) (Cat. No. 4665), Anti-RECK (Cat. No. 3433), Anti-MMP-9 (Cat. No. 2270), Anti-MMP-2

(Cat. No. 4022), Anti-N-Cadherin (Cat. No. 13116), Anti-E-Cadherin (Cat. No. 3195), Anti-Slug (Cat. No. 9585), Anti-Snail (Cat. No. 3879), Anti-Claudin-1 (Cat. No. 4933), Anti-Phospho-LIMK1 (Thr508)/LIMK2 (Thr505) (Cat. No. 3841), Anti-GAPDH (Cat. No. 5174), Anti-Bax (Cat. No. 2772), Anti-Bcl-2 (Cat. No. 3498), Anti-Caspase 9 (Cat. No. 9502), and Anti-Phospho-Cofilin (Ser3) (Cat. No. 3313) were purchased from CST. All antibodies for Western blots were diluted 1000 times, except profilin (10000 times).

Cell viability assay

Cell viability was assessed using the CCK-8 assay. Cells were seeded at a density of 2000 cells/well in 96-well plates and incubated for 24 hrs for adherence. Following treatment with different concentrations of eupatilin (0, 40, 80, 160, and 320 μM) for 8, 16, 24, 48, and 72 hrs, 10 μL of CCK-8 reagent was added to each well and incubated for 1–2 hrs at 37°C. The optical density (OD) value was read at 450 nm using Thermo Fisher Scientific SkanIt Software 3.1 for Multiskan GO. The viability rate of cells =(the OD values of treated groups/the OD values of the control group) × 100%.

Flow cytometry analysis of the cell cycle

Cells were seeded at a density of 1×10^6/mL and cultured in a 6-well plate. After adherence, the cells were synchronized for 12 hrs with serum-free media and treated with 0, 40, 80, or 160 μM eupatilin for 24 hrs. Cells were harvested and fixed in 75% cold ethanol for 12 hrs and washed twice with PBS. Cells were incubated with 100 mg/mL RNase A and 50 mg/mL propidium iodide at 37°C for 30 mins. The cell cycle was analyzed by flow cytometry.

Cell scratch test

All cell lines were cultured in 6-well plates. Cells were grown to 85% confluence, scratched in each well with a new 1 mL pipette tip, washed twice with PBS to remove the scraped cells, and treated with eupatilin for 24 or 48 hrs. Images were taken and the gap distance was quantified using Image J 1.48V software.

Cell invasion assay

Transwell inserts were coated with matrigel (1:8 dilution with serum-free medium). Six hundred milliliters of DMEM with 20% FBS and eupatilin at different concentrations (0, 40, 80, or 160 μM) were added to the lower transwell compartment.

Four cell lines were seeded to the upper compartment at a density of 1×10^5/μL (200 μL/well). After the cells were incubated for 24 hrs, the residual matrigel above the chamber was wiped with a cotton swab. The chamber was fixed with paraformaldehyde and stained with crystal violet, and four different fields were randomly selected for cell counting.

Western blot

U251MG cells were harvested after treatment with 0, 40, 80, or 160 μM eupatilin for 24 hrs. Protein was extracted after cell lysis and protein concentration was measured. Samples were separated by electrophoresis on a 12% SDS-PAGE gel (30 mg total protein/lane). After transfer to a PVDF membrane, proteins were blocked with 5% BSA for 1 hr and the membrane was incubated overnight at 4°C with the primary antibody. Membranes were washed three times with TBST and incubated with goat anti-mouse/rabbit secondary antibody for 2 hrs at room temperature. After washing with TBST, membranes were scanned by ECL and analyzed using a Bio-Rad gel imaging system.

Immunofluorescence

U251MG cells were plated in 12-well plates and treated with 0 or 160 μM eupatilin for 24 hrs, and cells were fixed with 4% formaldehyde diluted in 1× PBS for 15 mins. The cells were washed three times with 1× PBS for 5 mins, samples were blocked in 5% BSA for 60 mins and incubated with the primary antibody overnight at 4°C. After washing with PBS, the secondary antibody was added at room temperature for 2 hrs in the dark, and the sample was analyzed by confocal microscopy.

Immunohistochemistry

Tumor tissue was fixed with 4% paraformaldehyde and paraffin sections were taken. Endogenous peroxidase was blocked with 3% H_2O_2 after high-pressure heat repair of the antigen. The sections were washed with PBST and blocked with 5% BSA for 1 hr at room temperature. After removing the blocking solution, the sections were incubated with primary antibody at 4°C overnight. Sections were washed with PBST, stained with the secondary antibody and developed with DAB. The colored sections with hematoxylin for 20 s. After washing, the sections were dehydrated using an alcohol gradient, and mounted.

Xenograft tumors in nude mice

A total of 30 female BALB/c nude mice were purchased from Shenzhen Huafukang Bioscience Co., Inc., Shenzhen,

China. U87 cells in the logarithmic growth phase were resuspended to a density of 2.5×10^5 cells/L with serum-free DMEM. A 100 μL cell suspension was subcutaneously injected into the left back of 6 nude mice using a microinjector. Tumor tissue was obtained from nude mice one week later and were cut into 1 mm³ slices. The tissue block was inoculated on the left back using ophthalmic tweezers. Seven days after inoculation, nude mice were assigned to a control group (daily intraperitoneal injection of 3% DMSO and 5% TWEEN-80 and normal saline), and an eupatilin group (daily intraperitoneal injection of 20 mg/kg eupatilin), with six mice in each group. Normal tumor-free nude mice were assigned to the control group and double drug dose group to study drug toxicity. The mice were intraperitoneally injected every other day and their body weight was calculated every 7 days for 30 consecutive days. After anesthetizing the nude mice, the drug efficacy group weighed the tumors of each group, and the drug toxicity group observed the drug toxicity by HE staining of each organ.

Statistical analysis

All experiments were repeated three times and the data were expressed as mean ± standard deviation. Shapiro–Wilk test was used to determine whether the data had a normal distribution. Two samples that conformed to a normal distribution were compared using an independent *T*-test. Multiple sample comparisons were analyzed by one-way ANOVA. Statistical analysis was performed using SPSS 17.0. *$p < 0.05$ was considered statistically significant.

Results

Eupatilin inhibits viability and proliferation of glioma cells

In the CCK-8 assay, we found that different concentrations of eupatilin treatment with different incubation times inhibited the viability and proliferation of four glioma cell lines U251MG, U118, T98G, and U87MG, to varying degrees. Among the cell lines, U251MG and U87MG were the most affected (Figure 1A).

Monoclonal experiments reflect two important traits of cell population dependence and proliferative capacity. A single tumor cell has the ability to proliferate indefinitely. To examine the effect of eupatilin on glioma cell population dependence and proliferation, U251MG and U87MG cells were counted and the same number of

cells were taken. Eupatilin was added to a final concentration of 0, 40, and 80 μM. The cells were incubated for 15 days in a conventional conditional incubator, with the medium changed every 5 days. After 15 days, the number of monoclonals formed in the eupatilin group was significantly lower than that in the control group, and the difference was concentration-dependent and statistically significant (Figure 1B and C), indicating that eupatilin inhibited the clonality of U251MG and U87MG.

Eupatilin has no effect on glioma cell apoptosis

Many drugs exert antitumor effects through mechanisms that promote cell apoptosis. Only one article has reported that eupatilin promotes apoptosis of glioma cells by inhibiting the Notch-1 signaling pathway.[15] However, after treatment of each cell line with eupatilin at different concentrations for 24 or 48 hrs, we did not detect eupatilin-promoted apoptosis using flow cytometry. To further confirm our experimental results, we used Western blot detection of Bax, bcl-2, and caspase-9 protein and found no significant difference (Figure S1).

Eupatilin significantly inhibits the cell cycle of glioma cells at the G1/S phase by affecting cell cycle regulatory proteins

Cell proliferation is accompanied by cell division and growth. To investigate how eupatilin inhibits the proliferation of glioma cells, we examined the periodic changes of individual cell lines. Cells were treated with different concentrations of eupatilin, and 30,000 cells were counted by flow cytometry. Eupatilin significantly affected the cell cycle of tumor cells causing arrest at the G1/S phase (Figure 2A). To further explore eupatilin's mechanism, we examined cell cycle regulatory proteins.

Cyclin E1 binds to cyclin E2 and activates CDK2.[16] Upregulation/activation of CDK inhibitors p21 Waf1/Cip1 and p27 Kip1 prevents cyclin E/CDK2 activation and thus arrests at G1/S (Figure 2C).[17] Western blotting revealed that eupatilin significantly decreased cyclin E2 and increased expression of p21 Waf/Cip1 (Figure 2B).

Many studies have shown that overexpression of cyclin A accelerates entry into S phase from G1 phase, leading to DNA replication. Cyclin A is essential for completion of the pre-mitotic phase.[18] Phosphorylation of histone H3 at Ser10, Ser28, and Thr11 sites is closely related to

A

B

C
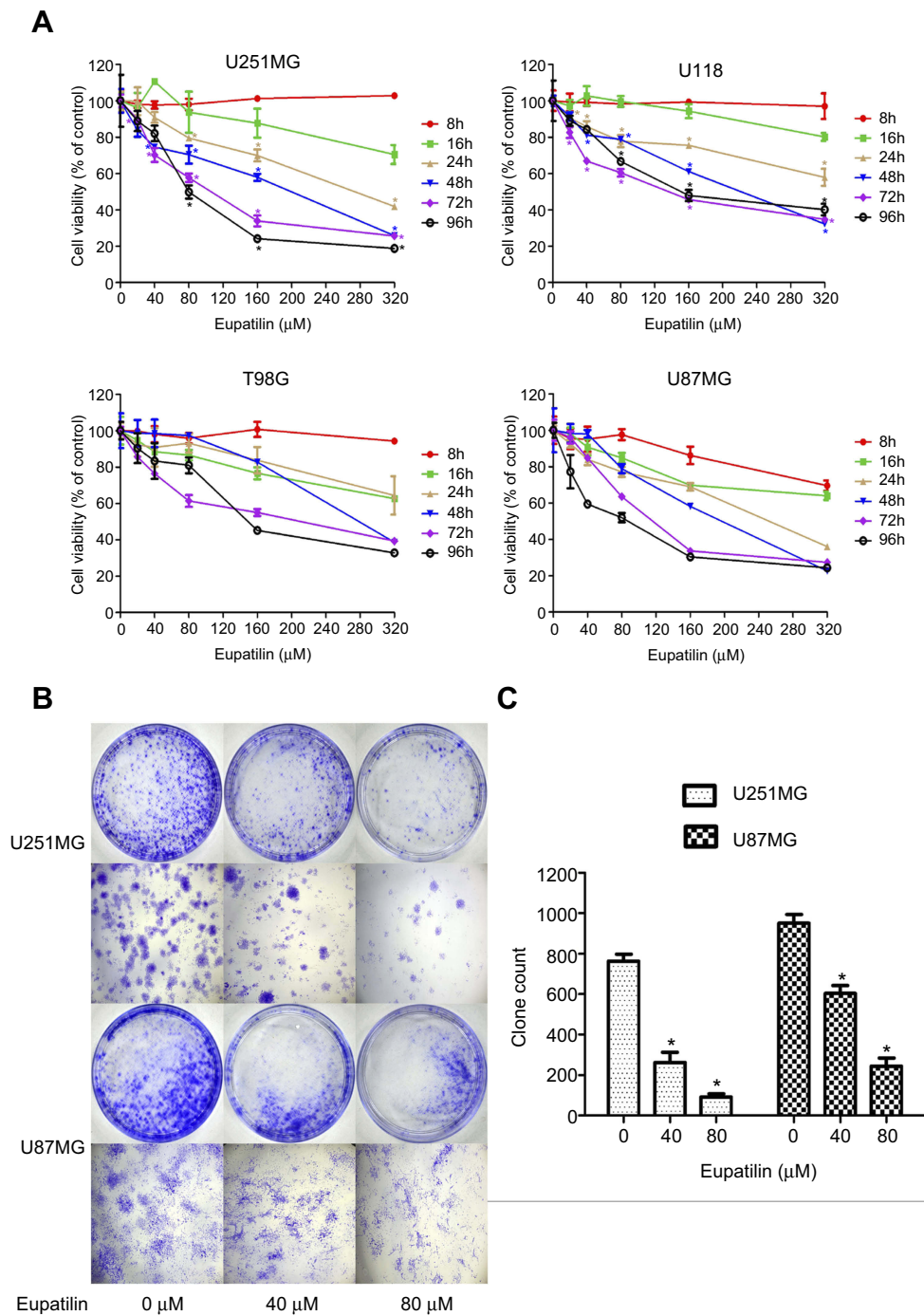
Figure 1 Eupatilin inhibits viability and proliferation of glioma cells. (A) Four cell lines were treated with different concentrations (0, 20, 40, 80, 160, 320 μM) of eupatilin for different time points (8, 16, 24, 48, 72, 96 hrs), and the optical density values were measured at a wavelength of 450 nm. The viability rate of cells = (the OD values of treated groups/the OD values of the control group) × 100%. (B) U251MG and U87MG count 5000 cells each and were treated with 0, 40, 80 μM eupatilin for 15 days. The ability of eupatilin-treated tumor cells to form cell clones is significantly weaker than untreated cells. (C) Count the number of clones in four random fields in each dish. Data are expressed as the mean ± standard deviation of three independent experiments. *$P<0.05$ vs the control group. Each experiment was repeated three times.

chromosomal concentration during mitosis and meiosis, affecting DNA synthesis (Figure 2C).[19,20] Eupatilin significantly reduced cyclin A and P-Histone H3[Ser10] expression (Figure 2B) and caused the cell cycle to be arrested at G1 phase.

It has been reported that p70 S6 kinase is a mitogen-activated Ser/Thr protein kinase that is required for cell growth and G1 cell cycle progression.[21] Ser411, Thr421, and Thr424 are located in the serine and proline-rich region of the pseudo-substrate domain. Phosphorylation of these
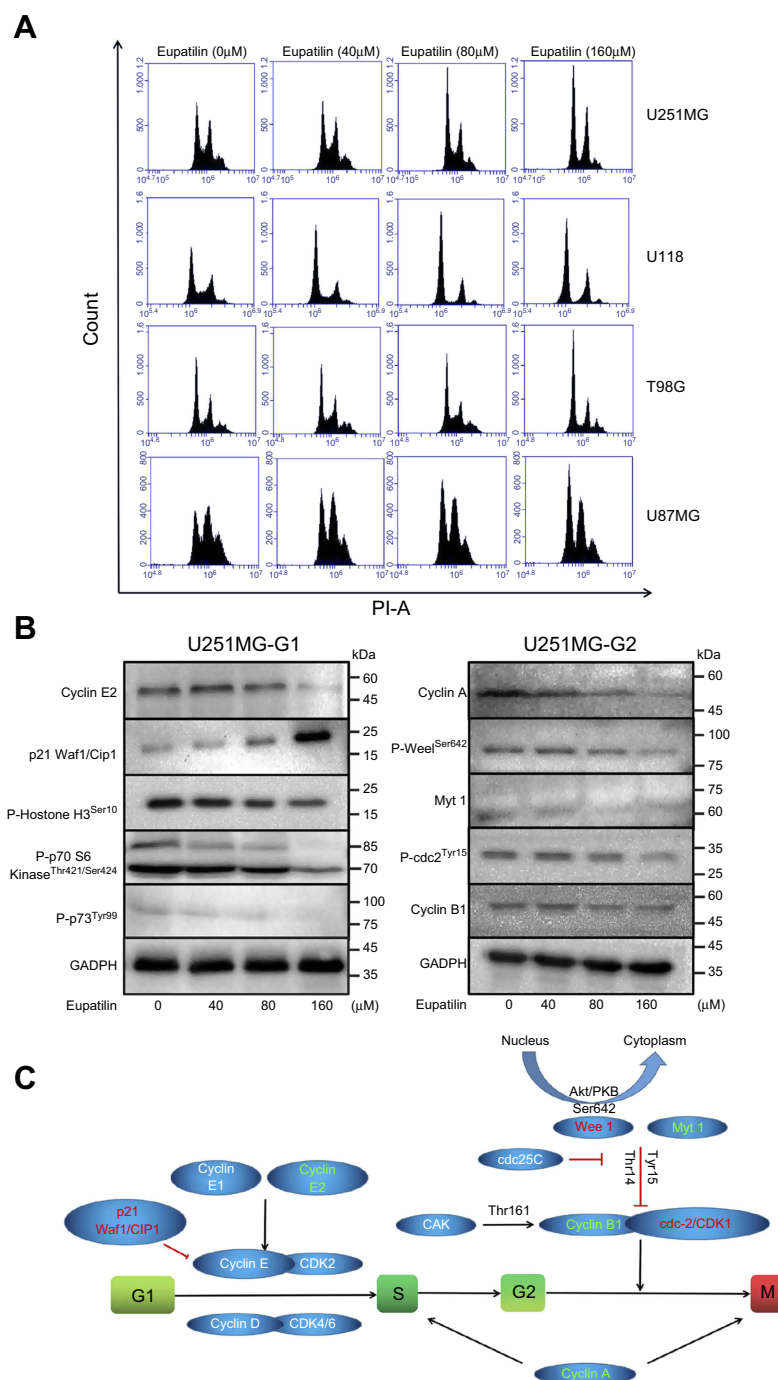
Figure 2 Eupatilin arrests the cell cycle of the glioma to the G1 phase and affects the expression of cell cycle regulatory proteins. (A) Four cell lines were synchronized for 12 hrs with serum-free medium, treated with different concentrations of eupatilin for 24 hrs, cells were harvested and the cell cycle was measured with flow cytometry. (B) U251 cells were treated with eupatilin for 24 hrs after synchronizing for 12 hrs, and the expression of regulatory proteins was detected by Western blot. GAPDH is used as a housekeeping protein to prove the equal loading in each lane of the electrophoresis and to normalize densitometric values of the other protein analyzed. Each experiment was repeated three times. (C) Schematic diagram of the role of cell cycle regulatory proteins in the process of cycle regulation.

residues is thought to activate p70 S6 kinase by abolishing inhibition of the pseudo-substrate.[21] Phosphorylation of p73 of Thr99 is required for the G1 phase of the cell cycle.[22] We found that eupatilin significantly decreased the expression of P-p70 S6 Kinase$^{Thr421/Ser424}$ and P-p73^{Tyr99} (Figure 2B).

Activation of cdc2/cdk1 during the G2/M conversion phase regulates the entry of all eukaryotic cells into mitosis. Activation is a multistep process that begins with a regulatory subunit and cyclin B1 binding to cdc2/cdk1 to form a mitotic promoting factor

(MPF). MPF remains in an inactive state until cdk activating kinase phosphorylates cdc2/cdk1 at its Thr161 site and cdc25C dephosphorylates at the Thr14/Tyr15 site.[23] Phosphorylation at the Tyr15 and Thr14 sites and inhibition of cdc2 are carried out by Wee1 and Myt1 protein kinases (Figure 2C).[24,25] Although Western blot showed P-Wee1[Ser642], Myt1 protein levels decreased, but there were no statistically significant changes in cyclin B1 and P-cdc2[Tyr15] in the MPF (Figure 2B). It indicated that the effect of eupatilin on G2 phase was weaker than that of G1 phase, and no significant changes in G2 phase were observed in flow cytometry experiments.

Eupatilin inhibits migration and invasion of glioma cells

A scratch wound healing assay was performed on four glioma cell lines U251MG, U118, T98G, and U87MG. Scratches were made in a 6-well plate with tips of uniform width, and cells were treated with 40 or 80 μM eupatilin and photographed under a microscope at 24 and 48 hrs to calculate the creep distance of cells on both sides of the scratch. It was found that eupatilin significantly inhibited cell migration in a dose-dependent manner (Figure 3A). There was no statistical significance when U87MG were cultured for 24 hrs. Cell migration distance inhibition rates were statistically significant when compared with the control group for all cell lines, apart from U87MG cultured for 24 hrs (Figure 3B). This was thought to be related to the growth characteristics of U87MG. In the transwell invasion assay, addition of eupatilin significantly inhibited the ability of each cell line to pass through the chamber at 24 hrs. Figure 3C is a microscopic photograph of the U251MG transwell chamber after crystal violet staining. Cell counts and statistical analysis of the four fields of the chamber were performed under a microscope, and Figure 3D shows that eupatilin inhibits the invasive ability of each cell line in a dose-dependent manner.

Eupatilin destroys the cytoskeleton of glioma cells via P-LIMK/cofilin pathway

After 48 hrs of treatment with eupatilin at 160 μM, U251MG cells became more elongated (Figure 4A). The cytoskeleton plays an important role in maintaining cell morphology and migration, and so, we hypothesized that eupatilin affects migration by affecting cytoskeletal proteins. F-actin was stained with Phalloidin-iFluor 488 reagent and observed by confocal microscopy. The microfilaments of untreated tumor cells showed intact filaments, while the microfilaments of the eupatilin treated group were broken and aggregated (Figure 4B). In order to eliminate the possibility that broken microfilament fragments were occluded by layer superposition, images of 0.4 μm thickness of each group were observed, with no broken microfilaments found in the control group (Figure 4B). The Golgi is an important organelle in the cell that is responsible for the processing and secretion of proteins. The transport of intracellular substances is closely related to the cytoskeleton. We used immunofluorescence to detect the Golgi marker protein GM130 and found that the Golgi of the control group were scattered in the cells, while the Golgi of the drug-treated group were detached from the microfilaments and had accumulated in the cells (Figure 4C). We also examined the cells' endoplasmic reticulum, and no significant changes were found (data not shown). We hypothesize that due to the attachment of the endoplasmic reticulum to the nuclear membrane, the nuclear membrane has a greater influence on its localization. In addition, G-actin polymerizes to form F-actin, and we found that the fluorescence intensity of G-actin in cells treated with eupatilin is statistically significant (Figure 4D and E).

Profilin is a conserved actin-binding protein that regulates the rate of actin polymerization by binding to actin monomers and promoting the exchange of ADP to ATP. Cofilin causes depolymerization at the minus end of microfilaments, thereby preventing their reassembly, but self-inhibition occurs after phosphorylation of Ser3.[26] LIM kinases (LIMK1 and LIMK2) are ser/thr kinases with two zinc finger motifs in their N-terminal regulatory domains. LIMK function downstream of the Rho family GTPases, PAK and ROCK.[27] PAK1 and ROCK phosphorylate LIMK1 or LIMK2 to increase LIMK activity at the conserved Thr508 or Thr505 residues in the activation loop.[28,29] The activated LIMK phosphorylates cofilin at its Ser3 residue inhibiting its depolymerization activity.[30] U251MG were treated with 160 μM eupatilin for different times. The effect on profilin was not obvious, but P-LIMK1[Thr508]/P-LIMK2[Thr505], P-cofilin[Ser3], and total cofilin decreased (Figure 4F). P-cofilin[Ser3] decreased more than total cofilin, and the ratio of cofilin/P-cofilin[Ser3] statistically increased (Figure 4G). It has been reported that phosphorylation of cofilin at the Ser3
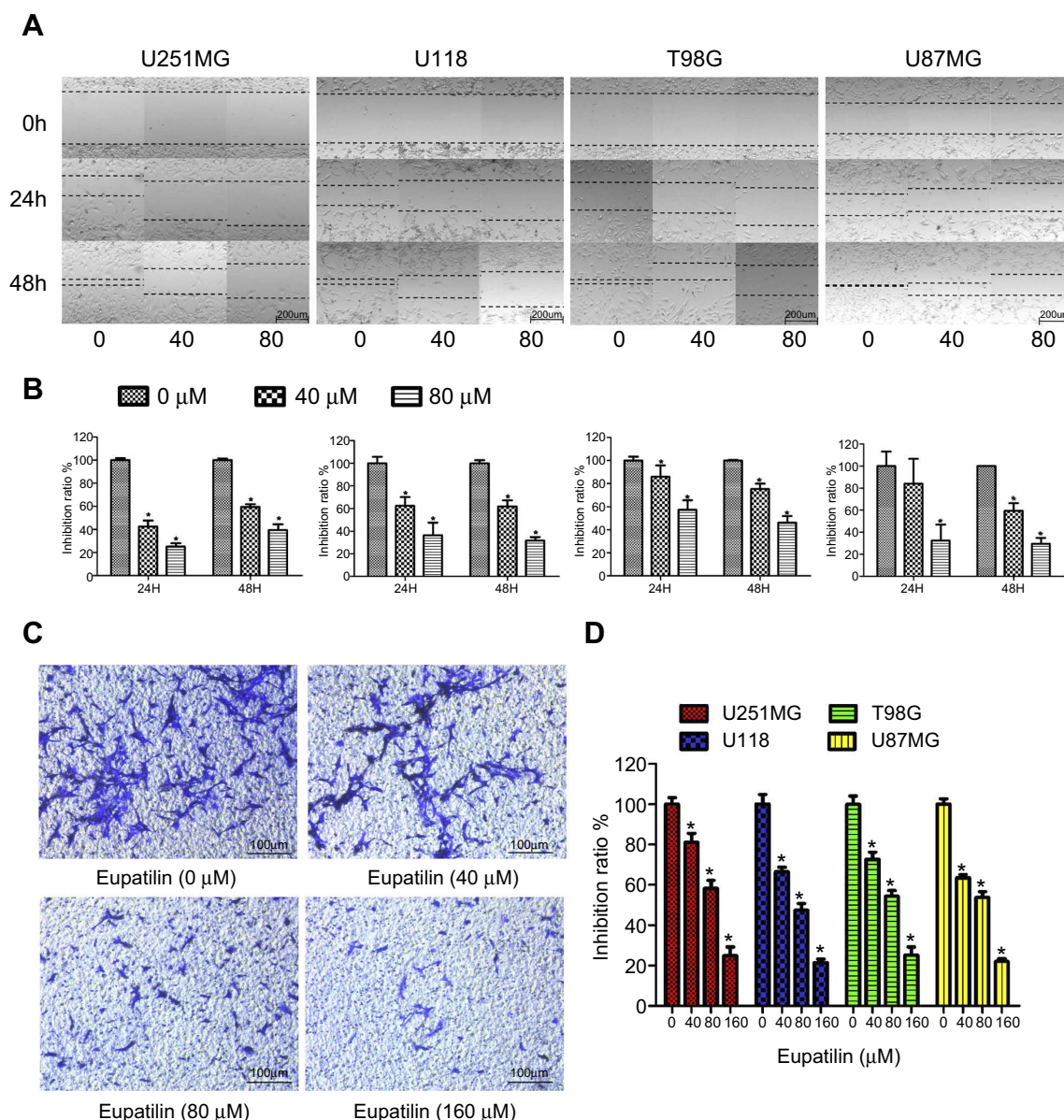
Figure 3 Eupatilin attenuates migration and invasion of glioma. (**A**) After scratching in a 6-well plate, the 4 cell lines were treated with different concentrations eupatilin for 48 hrs and photographed at 0, 24, and 48 hrs, respectively. (**B**) Statistical analysis of cell spacing on both sides. (**C**) U251MG cells were cultured for 24 hrs under conditions containing 20% serum and different concentrations of eupatilin under the chamber and stained with crystal violet and photographed with a microscope. (**D**) Counting the number of cells in three different random fields of each chamber under the microscope. Data are expressed as the mean ± standard deviation of three independent experiments. *P<0.05 vs the control group. Each experiment was repeated three times.

site also regulates the translocation of cofilin from the nucleus to the cytoplasm, and so we further explored whether eupatilin affects the localization of cofilin. Although Western blot analysis showed a decrease in total cofilin protein, immunofluorescence confirmed a decrease in the nucleus and an increase in the cytoplasm (Figure 4H). P-cofilin[Ser3] decreased in both the nucleus and the cytosol (Figure 4I). These results indicated that the eupatilin destroys the cytoskeleton of glioma cells via P-LIMK/cofilin pathway, thereby affecting the migration of tumor cells.

Eupatilin attenuates the invasive ability of glioma cells by affecting EMT and RECK/MMP pathways

Transwell experiments revealed that eupatilin inhibits glioma cell invasion. Dil staining showed that cell membrane connections between the cells in the eupatilin group were weakened (Figure 5A). Tight junctions form a continuous fluid barrier between the epithelial and endothelial cells, which are composed of claudin and occludin and connect to the cytoskeleton. The
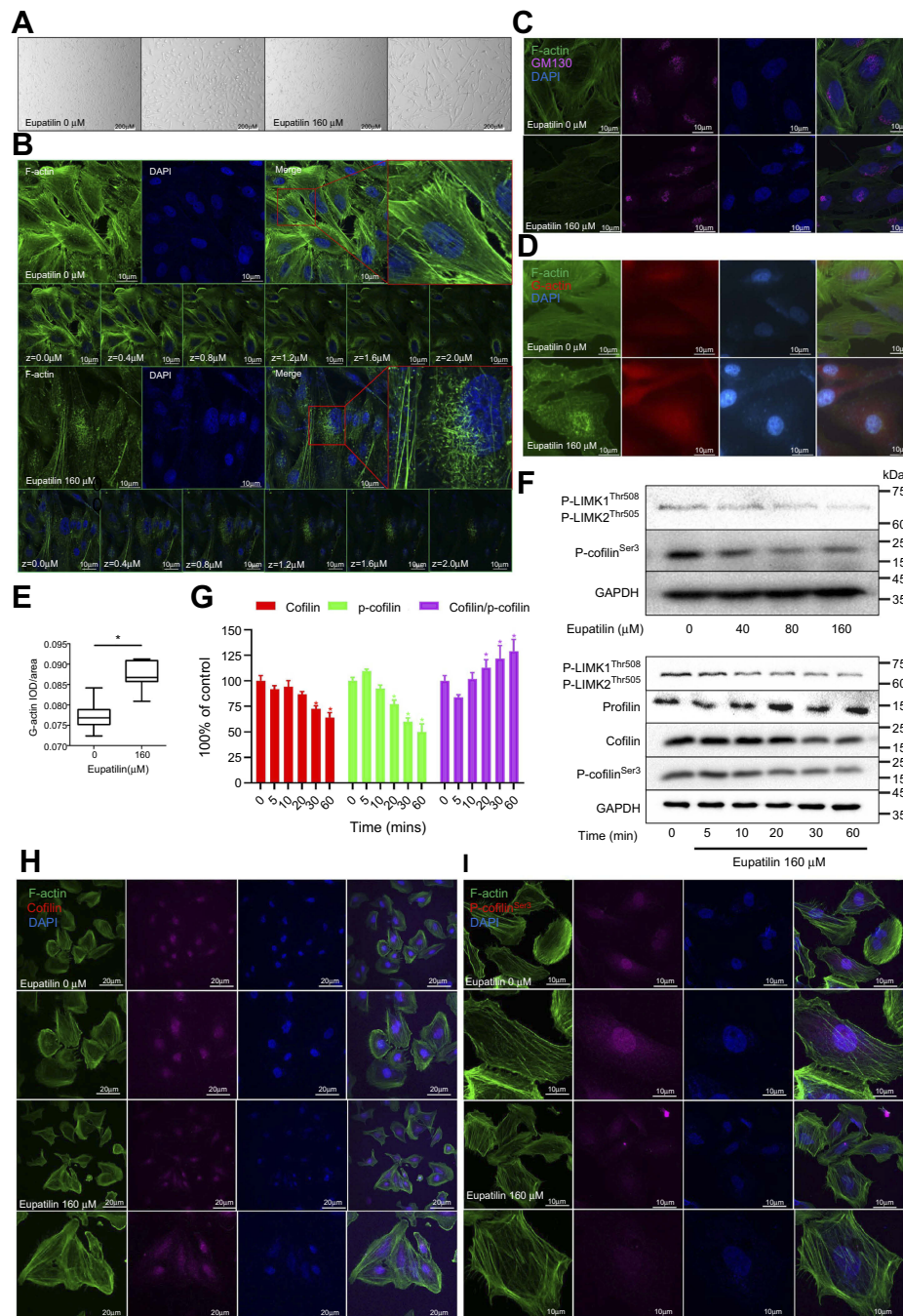
Figure 4 Eupatilin disrupts the cytoskeleton and affects intracellular relocalization of cofilin via the p-LIMK/cofilin pathway. (**A**) Treatment of U251MG cells with 160 µM eupatilin for 24 hrs and photographing with an inverted microscope. (**B**) F-actin was stained with Phalloidin-iFluor 488, and the microfilament shape of each layer (0.4 um) and superimposed layer (2.0 um) was observed by confocal microscopy, DAPI: 405 nm. (**C**) Immunofluorescence detection of Golgi marker protein GM130 (wavelength: 647 nm). (**D**) The expression of G-actin was detected by immunofluorescence (wavelength: 555 nm), and the optical density value (**E**) was calculated and statistically analyzed with image J. (**F**) Western detection of protein expression in the p-LIMK/cofilin pathway after treatment of U251MG with different time gradients and eupatilin concentration gradients. GAPDH is used as a housekeeping protein to prove the equal loading in each lane of the electrophoresis and to normalize densitometric values of the other protein analyzed. (**G**) Statistical analysis of Cofilin, p-cofilinSer3, and cofilin/p-cofilinSer with Quantity One after treatment with 160 µM eupatilin for different times, and the difference was statistically significant. *$P<0.05$ vs the control group. U251MG was treated with 160 µM eupatilin for 24 hrs, and p-cofilinSer3 (**I**) and cofilin (**H**) were stained to observe intracellular localization (wavelength: 647 nm). Each experiment was repeated three times.

claudin family consists of 23 integral membrane proteins that vary among tissue types and determine the strength and characteristics of the epithelial barrier. However, no significant change in claudin-1 was observed after 48 hrs of drug exposure in U251MG cells (Figure 5B).

Epithelial–mesenchymal transition (EMT) is one of the important and classical features of tumor transformation

from benign to malignant. We explored whether eupatilin inhibits the invasiveness of glioma by affecting EMT. The classical cadherin subfamily includes N-, P-, R-, B-, and E-cadherin. The adhesion junction is a cellular structure on the top surface of polarized epithelial cells. N-cadherin cooperates with the FGF receptor, resulting in MMP-9 overexpression and cell invasion.[31] Snail is a zinc finger transcription factor that inhibits E-cadherin transcription. Slug (SNAI2) is a widely expressed transcriptional repressor protein and a member of the Snail family of zinc finger transcription factors. Like Snail, Slug binds to the E-cadherin promoter region to inhibit transcription during development.[32,33] Loss of E-cadherin and upregulation of N-cadherin expression in cells is called "cadherin conversion/EMT". We found that both Slug and Snail expression was upregulated after drug treatment, while the expression of E-cadherin and N-cadherin decreased (Figure 5B), disrupting the process of cadherin conversion in the tumor cells. As a transcriptional repressor, whether upregulated Slug and its family member Snail reduce tumor invasiveness by reducing the expression of other proteins remains to be studied.

RECK is a GPI-anchored membrane glycoprotein that negatively regulates members of the MMP family and acts as a transforming inhibitor. MMP is a family of proteases that target many extracellular proteins, including growth factors, cell surface receptors, and adhesion molecules.[34,35] Among these family members, MMP-2, MMP-3, MMP-7, and MMP-9 are considered important factors for normal tissue remodeling in embryonic development, injury repair, cancer invasion, angiogenesis, carcinogenesis, and apoptosis. Studies have shown that MMP activity is associated with cancer progression. RECK negatively regulates the MMP family. Although eupatilin caused downregulation of RECK, it also disrupted the process by which RECK regulates downstream proteins. MMP-2 expression also decreased while MMP-9 expression did not change significantly (Figure 5B). This shows that eupatilin not only affects the upstream protein RECK, but also acts on the regulation of MMP family by RECK, thereby attenuating the invasiveness of gliomas.

Eupatilin inhibits growth of human gliomas in nude mice xenograft models

To further explore the effects of eupatilin on tumors in vivo, we subcutaneously implanted 4-week-old nude mice with U87MG tumors. One week later, nude mice
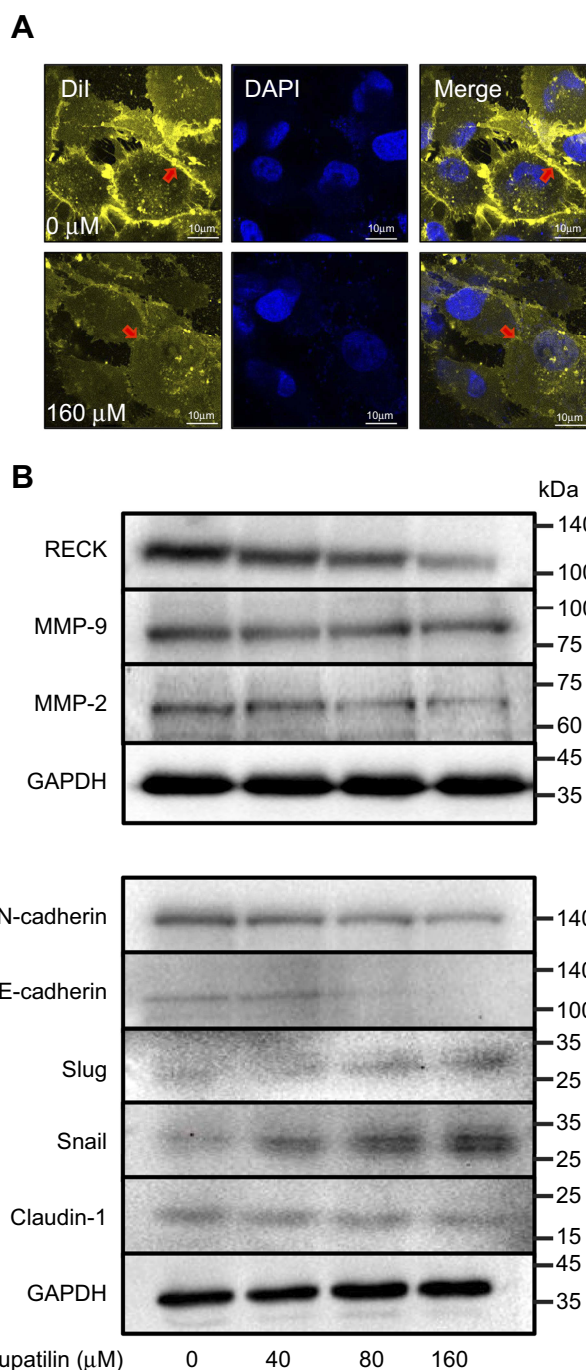

Figure 5 Eupatilin affects protein expression in EMT and RECK/MMP pathways. (**A**) Cell membrane of U251MG was stained with DiI (20 μM) for 30 mins after 24 hrs of treatment with eupatilin (wavelength: 555 nm). (**B**) Western blot detects the expression of related proteins in EMT and RECK/MMP pathways. GAPDH is used as a housekeeping protein to prove the equal loading in each lane of the electrophoresis and to normalize densitometric values of the other protein analyzed. Each experiment was repeated three times.

with the same tumor size were selected and randomly divided into two groups. The experimental group was given a dose of 20 mg/kg eupatilin by intraperitoneal injection. The control group was injected with the same amount of solvent used for eupatilin (H$_2$O, DMSO,

TWEEN-80). The drug was administered every two days, mice were weighed every 7 days, and the dose was adjusted accordingly. After 1 month of administration, the nude mice were anesthetized. The tumor sizes of the nude mice in the experimental group were significantly smaller than those of the control group (Figure 6A). Both groups of nude mice gained weight within 1 month, but the difference was not statistically significant (Figure 6B). We extracted the tumor and weighed it, and the difference between the two groups was statistically significant (Figure 6C and D). In addition, in order to verify the drug toxicity of eupatilin on nude mice, double doses were administered simultaneously within the experimental group. One month later, the brain, liver, and kidney tissues of nude mice were stained with HE and found to be free of drug toxicity (Figure 6E).

Tumor tissues were also stained with HE. We found no significant differences in the morphology of the two groups of tumor cells, which had the characteristic nucleus of tumor cells (Figure 6F). By immunohistochemistry, tumor tissue injected with eupatilin had less P-cofilin[Ser3] than the control, which is consistent with the results of our in vivo experiments. Additionally, it is interesting that tumor tissue injected with eupatilin had less Ki-67, an indicator of tumor proliferation and prognosis, than the control (Figure 6G).

Discussion

Current studies have revealed that eupatilin has anticancer effects on grade IV glioblastoma cells. This is demonstrated by its inhibition of tumor cell viability, proliferation, migration, and invasion. In addition, the cell cycle is arrested at G1/S phase after eupatilin treatment by regulating cell cycle regulatory proteins. Eupatilin also disrupts cytoskeletal microfilaments via the P-LIMK/cofilin pathway and also affects the RECK/MMP pathway and EMT processes to inhibit glioma invasion. Eupatilin also demonstrated the ability to inhibit glioma growth in xenograft nude mice.

Tumor cell proliferation is one of the basic biological characteristics of tumor formation. Therefore, inhibition of tumor proliferation has become the goal of cancer treatment. This study determined that eupatilin inhibits glioma cell proliferation and viability in a dose-dependent manner. Furthermore, eupatilin also inhibits the proliferation of human aortic smooth muscle cells[36] and ras-transformed human mammary epithelial cells.[37] Cell proliferation must be accompanied by cell division, and cyclin regulates the

cell cycle. We found that eupatilin treatment arrests glioma cells at G1/S phase by regulating the expression of cyclin E2, p21 Waf/Cip1, and other proteins. In addition, eupatilin inhibits the growth of human endometrial cancer cells by upregulating p21 to arrest the cell cycle at G2/M phase. Although eupatilin has different effects on different tumors, its effect on the cell cycle has been proven.

Inducing apoptosis is an important method for treating cancer. Studies have found that eupatilin may induce apoptosis of human promyelocytic leukemia cells[38] and gastric cancer cells.[39] The only study on gliomas showed that eupatilin promotes glioma cell apoptosis in a concentration-dependent manner.[15] However, due to factors such as the experimental environment, drug batches, etc., we did not observe this proapoptotic effect of eupatilin on glioma cell lines by flow cytometry or Western blot.

Reducing tumor metastasis is also a popular mechanism used in cancer treatment as high metastasis rates often lead to poor prognosis. Migration and invasion of tumor cells should be inhibited to reduce tumor metastasis. We found that eupatilin reduces the invasion and migration of glioma cells in a dose-dependent manner, which is consistent with the study of eupatilin as a chemo-preventive and anti-metastatic agent for human gastric cancer.[12] In addition, eupatilin inhibits angiogenesis-mediated human hepatocyte metastasis by reducing MMP-2 and VEGF signaling.[14]

Three mammalian cofilin family members, ADF, cofilin-1 non-muscle type, and cofilin-2 muscle type, are important in regulating F-actin depolymerization and remodeling. Studies have shown that LIM kinases, LIMK1 and LIMK2, and TES kinases, TESK1 and TESK2, specifically phosphorylate the N-terminal Ser3 site of cofilin, thereby inhibiting its actin binding activity.[26] Phosphorylation of LIMK at Thr508 and Thr505 increased its kinase activity, while eupatilin reduced the phosphorylation of LIMK, thereby attenuating phosphorylation of cofilin at its Ser3 site.[28,29] Although we found that total cofilin also decreased, the ratio of cofilin/P-cofilin[ser3] increased. Immunohistochemical results of tumor tissue also showed lower P-cofilin content after eupatilin treatment. In addition, studies have demonstrated that phosphorylation at Ser3 also regulates the process by which cofilin translocates from the nucleus to the cytoplasm. Our immunofluorescence results also confirmed that cofilin decreased in the nucleus after eupatilin treatment but increased in the cytoplasm. In general, eupatilin disrupts the cytoskeleton through the
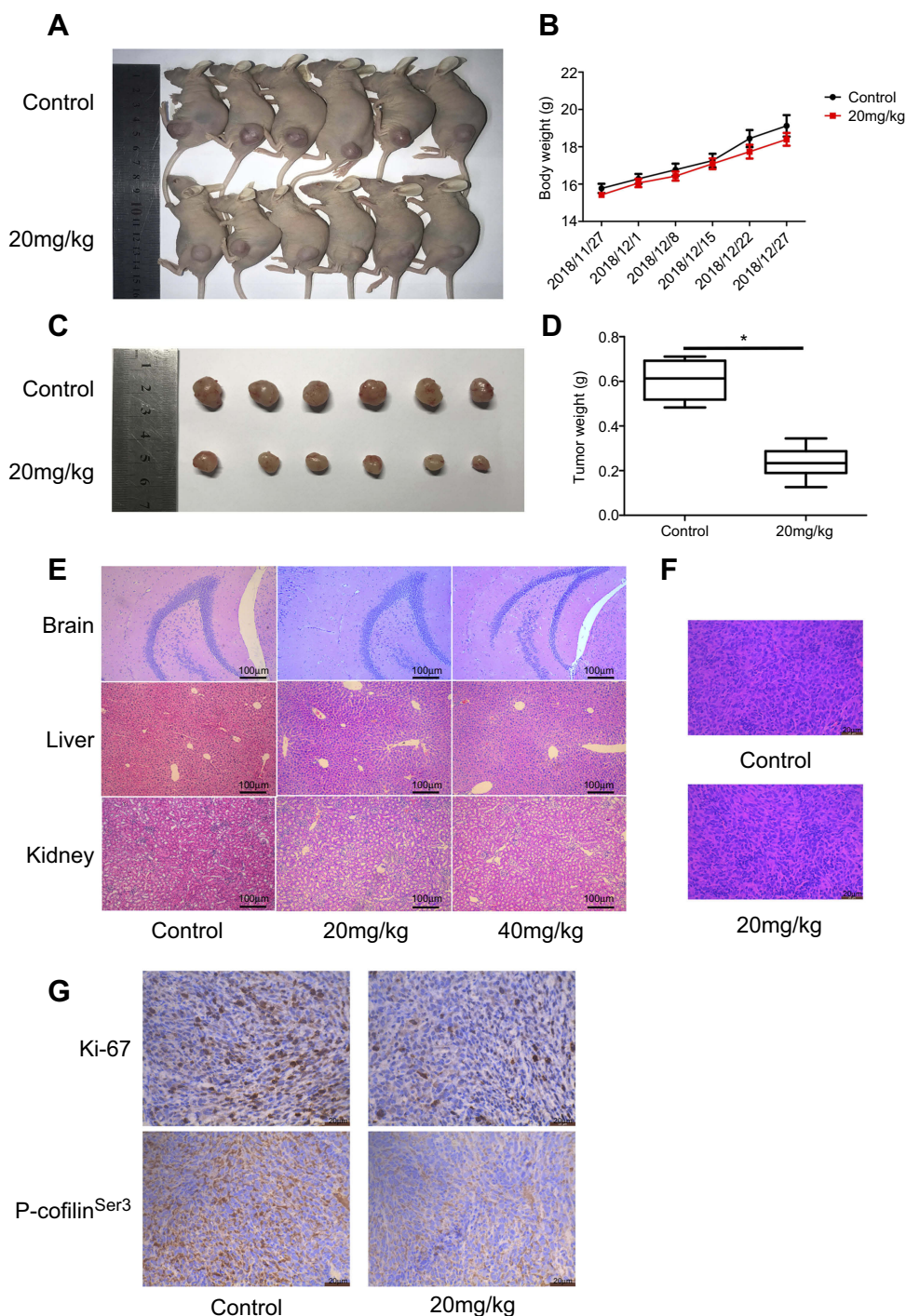
Figure 6 Eupatilin inhibits the growth of glioma in xenografted nude mice. Nude mice with uniform tumor size were injected intraperitoneally with 20 mg/kg eupatilin every other day. The body weight was calculated every 7 days for 30 consecutive days. There was a significant difference in tumor volume (**A** and **C**) and weight (**D**) in nude mice after 1 month of continuous injection, and the difference was statistically significant. *P<0.05 vs the control group. There was no significant difference in body weight between the two groups (**B**). The drug toxicity group observed the drug toxicity by HE staining of each organ (**E**). Tumor tissues were stained with HE (**F**). P-cofilin[Ser3] and Ki-67 were stained with immunohistochemistry (**G**).

p-LIMK/cofilin pathway, thereby inhibiting the migration of tumor cells.

No significant change in claudin-1 was observed after 48 hrs of drug exposure in U251MG cells. We suggest that eupatilin does not affect the tight junction between cells.

Additionally, the process of E-Cadherin decline and N-Cadherin increase in epithelial cells is called "EMT". We found that expression of the transcriptional repressor protein Slug and its family member Snail was upregulated after eupatilin treatment, while expression of E-cadherin

and N-cadherin decreased. Although drug treatment did not inhibit the critical step in EMT, ie, E-Cadherin decline, it disrupted the overall process of EMT. RECK negatively regulates the MMP family. RECK expression was downregulated after eupatilin treatment, but MMP-2 expression decreased, while MMP-9 expression did not change significantly (Figure 5B). Therefore, we hypothesized that eupatilin not only affects the expression of RECK itself but also inhibits the regulation of RECK, thereby attenuating the invasion ability of glioma. Interestingly, studies have shown that N-Cadherin cooperates with FGF receptors, leading to MMP-9 overexpression and cell invasion. We observed upregulated Slug and downregulated N-Cadherin. Whether eupatilin reduces RECK expression through the Slug family members or directly affects RECK remains to be studied. In addition, studies have shown that eupatilin inhibits proliferation, migration, and invasion and induces apoptosis by inhibiting the Notch-1 signaling pathway.[15]

A weakened invasive ability means a good prognosis for patients.[40] Eupatilin attenuates the invasiveness of gliomas, and so we predict that it will improve patient prognosis. In view of the difficulty of clinical trials, we used immunohistochemistry to detect the Ki-67 index, which was consistent with our predictions. Tumors in nude mice injected with eupatilin showed lower Ki-67. This means that eupatilin may improve the prognosis of malignant glioma. Ki-67 is ubiquitously expressed in proliferating cells,[41] and less Ki-67 means a weaker proliferative capacity of the tumor, which is consistent with the results of in vivo experiments with CCK-8 and monoclonal experiment.

Conclusion

In conclusion, we found that eupatilin inhibits proliferation, migration, and invasion of glioma cells and also inhibits tumor growth in nude mice. Therefore, the emergence of eupatilin brings a new dawn for glioma patients.

Ethics approval

All experiments involving the animals were approved by the Institutional Animal Ethics Committee of the Seventh Medical Center of the Chinese People's Liberation Army General Hospital. All procedures performed in the study involving the animals followed "The Guide for the Care and Use of Laboratory Animals" guidelines for animal welfare.

Acknowledgments

Disclosure

The authors report no conflicts of interest in this work.

References

1. Ostrom QT, Gittleman H, Farah P, et al. CBTRUS statistical report: primary brain and central nervous system tumors diagnosed in the United States in 2006–2010. *Neuro-Oncology.* 2013;15:ii1–ii56. doi:10.1093/neuonc/not151
2. Posti JP, Bori M, Kauko T, et al. Presenting symptoms of glioma in adults. *Acta Neurol Scand.* 2015;131(2):88–93. doi:10.1111/ane.12285
3. Borghei-Razavi H, Shibao S, Schick U. Prechiasmatic transection of the optic nerve in optic nerve glioma: technical description and surgical outcome. *Neurosurg Rev.* 2017;40(1):1–7. doi:10.1007/s10143-016-0709-8
4. Corradini S, Hadi I, Hankel V, et al. Radiotherapy of spinal cord gliomas: a retrospective mono-institutional analysis. *Strahlentherapie Und Onkologie.* 2016;192(3):139–145. doi:10.1007/s00066-015-0917-0
5. Kinno R, Ohta S, Muragaki Y, Maruyama T, Sakai KL. Left frontal glioma induces functional connectivity changes in syntax-related networks. *Springerplus.* 2015;4(1):317. doi:10.1186/s40064-015-1104-6
6. Zinn PO, Colen RR, Kasper EM, Jan-Karl B. Extent of resection and radiotherapy in GBM: a 1973 to 2007 surveillance, epidemiology and end results analysis of 21,783 patients. *Int J Oncol.* 2013;42 (3):929–934. doi:10.3892/ijo.2013.1770
7. Kreth FW, Thon N, Simon M, et al. Gross total but not incomplete resection of glioblastoma prolongs survival in the era of radiochemotherapy. *Ann of Oncol.* 2013;24(12):3117–3123. doi:10.1093/annonc/mdt388
8. Chen G, Yue Y, Qin J, Xiao X, Ren Q, Xiao B. Plumbagin suppresses the migration and invasion of glioma cells via downregulation of MMP-2/9 expression and inaction of PI3K/Akt signaling pathway in vitro. *J Pharmacol Sci.* 2017;134(1):59–67. doi:10.1016/j.jphs.2017.04.003
9. Lin TH, Kuo HC, Chou FP, Lu FJ. Berberine enhances inhibition of glioma tumor cell migration and invasiveness mediated by arsenic trioxide. *BMC Cancer.* 2008;8(1):1–15. doi:10.1186/1471-2407-8-1
10. Choi EJ, Lee S, Chae JR, Lee HS, Jun CD, Kim SH. Eupatilin inhibits lipopolysaccharide-induced expression of inflammatory mediators in macrophages. *Life Sci.* 2011;88(25):1121–1126. doi:10.1016/j.lfs.2011.04.011
11. Cheong JH, Hong SY, Zheng Y, Noh SH. Eupatilin inhibits gastric cancer cell growth by blocking STAT3-mediated VEGF expression. *J Gastric Cancer.* 2011;11(1):16–22. doi:10.5230/jgc.2011.11.1.16
12. Park BB, Yoon JS, Kim ES, et al. Inhibitory effects of eupatilin on tumor invasion of human gastric cancer MKN-1 cells. *Tumor Biol.* 2013;34(2):875–885. doi:10.1007/s13277-012-0621-y
13. Cho JH, Lee JG, Yang YI, et al. Eupatilin, a dietary flavonoid, induces G2/M cell cycle arrest in human endometrial cancer cells. *Food Chem Toxicol.* 2011;49(8):1737–1744. doi:10.1016/j.fct.2011.04.019
14. Jun YP, Do HP, Youngsic J, et al. Eupatilin inhibits angiogenesis-mediated human hepatocellular metastasis by reducing MMP-2 and VEGF signaling. *Bioorg Med Chem Lett.* 2018;28(19):3150–3154.
15. Wang Y, Hou H, Li M, Yang Y, Sun L. Anticancer effect of eupatilin on glioma cells through inhibition of the Notch-1 signaling pathway. *Mol Med Rep.* 2016;13(2):1141–1146. doi:10.3892/mmr.2015.4671

16. Lauper N, Beck AR, Cariou S, et al. Cyclin E2: a novel CDK2 partner in the late G1 and S phases of the mammalian cell cycle. *Oncogene*. 1998;17(20):2637. doi:10.1038/sj.onc.1202015

17. Pestell R, Albanese C, Reutens AT, Segall J, Lee R, Arnold A. The cyclins and cyclin-dependent kinase inhibitors in hormonal regulation of proliferation and differentiation. *Endocr Rev*. 1999;20(4):501–534. doi:10.1210/edrv.20.4.0373

18. Zindy F, Lamas E, Chenivesse X, et al. Cyclin A is required in S phase in normal epithelial cells. *Biochem Biophys Res Commun*. 1992;182(3):1144–1154.

19. Preuss U, Landsberg G, Scheidtmann KH. Novel mitosis-specific phosphorylation of histone H3 at Thr11 mediated by Dlk/ZIP kinase. *Nucleic Acids Res*. 2003;31(3):878–885. doi:10.1093/nar/gkg176

20. Goto H, Tomono Y, Ajiro K, et al. Identification of a novel phosphorylation site on histone H3 coupled with mitotic chromosome condensation. *J Bio Chem*. 1999;274(36):25543–25549.

21. Lane HA, Fernandez A, Lamb NJC, Thomas G. p70 s6k function is essential for G1 progression. *Nature*. 1993;363(6425):170–172. doi:10.1038/363170a0

22. Satija YK, Das S. Tyr99 phosphorylation determines the regulatory milieu of tumor suppressor p73. *Oncogene*. 2015;35(4):513. doi:10.1038/onc.2015.111

23. Lorca T, Labbé JC, Devault A, et al. Dephosphorylation of cdc2 on threonine 161 is required for cdc2 kinase inactivation and normal anaphase. *Embo J*. 1992;11(7):2381–2390.

24. Watanabe N, Broome M, Hunter T. Regulation of the human WEE1Hu CDK tyrosine 15-kinase during the cell cycle. *Embo J*. 1995;14(9):1878–1891.

25. Mcgowan CH, Russell P. Human Wee1 kinase inhibits cell division by phosphorylating p34cdc2 exclusively on Tyr15. *Embo J*. 1993;12(1):75–85.

26. Gahan PB. The cell: a molecular approach (3rd edn) G. M. Cooper and R. E. Hausman, Palgrave-Macmillans Global Academic Publishing, 713 pp., ISBN 0-87893-214-3 (2004). *Cell Biochem Funct*. 2010;23(3):222.

27. Maekawa M, Ishizaki T, Boku S, et al. Signaling from Rho to the actin cytoskeleton through protein kinases ROCK and LIM-kinase. *Science*. 1999;285(5429):895. doi:10.1126/science.285.5429.895

28. Sumi T, Matsumoto K, Nakamura T. Specific activation of LIM kinase 2 via phosphorylation of threonine 505 by ROCK, a Rho-dependent protein kinase. *J Biol Chem*. 2001;276(1):670–676. doi:10.1074/jbc.M007074200

29. Ohashi K, Nagata K, Maekawa M, Ishizaki T, Narumiya S, Mizuno K. Rho-associated kinase ROCK activates LIM-kinase 1 by phosphorylation at threonine 508 within the activation loop. *J Bio Chem*. 2000;275(5):3577. doi:10.1074/jbc.275.5.3577

30. Arber S, Barbayannis FA, Hanser H, et al. Regulation of actin dynamics through phosphorylation of cofilin by LIM-kinase. *Nature*. 1998;393(6687):805–809. doi:10.1038/31729

31. Hazan RB, Qiao R, Keren R, Badano I, Suyama K. Cadherin switch in tumor progression. *Ann N Y Acad Sci*. 2010;1014(1):155–163. doi:10.1196/annals.1294.016

32. Yokoyama K, Kamata N, Hayashi E, et al. Reverse correlation of E-cadherin and snail expression in oral squamous cell carcinoma cells in vitro. *Oral Oncol*. 2001;37(1):65–71.

33. Yokoyama K, Kamata N, Fujimoto R, et al. Increased invasion and matrix metalloproteinase-2 expression by Snail-induced mesenchymal transition in squamous cell carcinomas. *Int J Oncol*. 2003;22(4):891.

34. Michiko E, Shunya K, Rei T, et al. The membrane-anchored MMP-regulator RECK is a target of myogenic regulatory factors. *Oncogene*. 2005;24(38):5850–5857. doi:10.1038/sj.onc.1208733

35. Shunya K, Chisa S, Yoko M, et al. Dual effects of the membrane-anchored MMP regulator RECK on chondrogenic differentiation of ATDC5 cells. *J Cell Sci*. 2007;120(5):849–857. doi:10.1242/jcs.03388

36. Joe Eun S, Eunjung L, Gwon SS, et al. Eupatilin, a major flavonoid of Artemisia, attenuates aortic smooth muscle cell proliferation and migration by inhibiting PI3K, MKK3/6, and MKK4 activities. *Planta Med*. 2013;79(12):1009–1016. doi:10.1055/s-0033-1350621

37. Do-Hee K, Hye-Kyung N, Tae Young O, Chang-Yell S, Young-Joon S. Eupatilin inhibits proliferation of ras-transformed human breast epithelial (MCF-10A-ras) cells. *J Environ Pathol Toxicol Oncol*. 2005;24(4):251–259.

38. Seo HJ, Surh YJ. Eupatilin, a pharmacologically active flavone derived from Artemisia plants, induces apoptosis in human promyelocytic leukemia cells ☆. *Mutat Res Genet Toxicol Environ Mutagen*. 2001;496(1):191–198. doi:10.1016/S1383-5718(01)00234-0

39. Kim MJ, Kim DHNa HK, Oh TY, Shin CY, Yj SPD. Eupatilin, a pharmacologically active flavone derived from artemisia plants, induces apoptosis in human gastric cancer (AGS) cells. *J Environ Pathol Toxicol Oncol*. 2005;24(4):261–270. doi:10.1615/JEnvironPatholToxicolOncol.v24.i4.30

40. Hongjiang L, Zhongqiang L, Erkun G. Knockdown of long noncoding RNA SPRY4-IT1 suppresses glioma cell proliferation, metastasis and epithelial-mesenchymal transition. *Int J Clin Exp Pathol*. 2015;8(8):9140.

41. Weigel MT, Dowsett M. Current and emerging biomarkers in breast cancer: prognosis and prediction. *Endocr Relat Cancer*. 2010;17(4):R245. doi:10.1677/ERC-10-0136
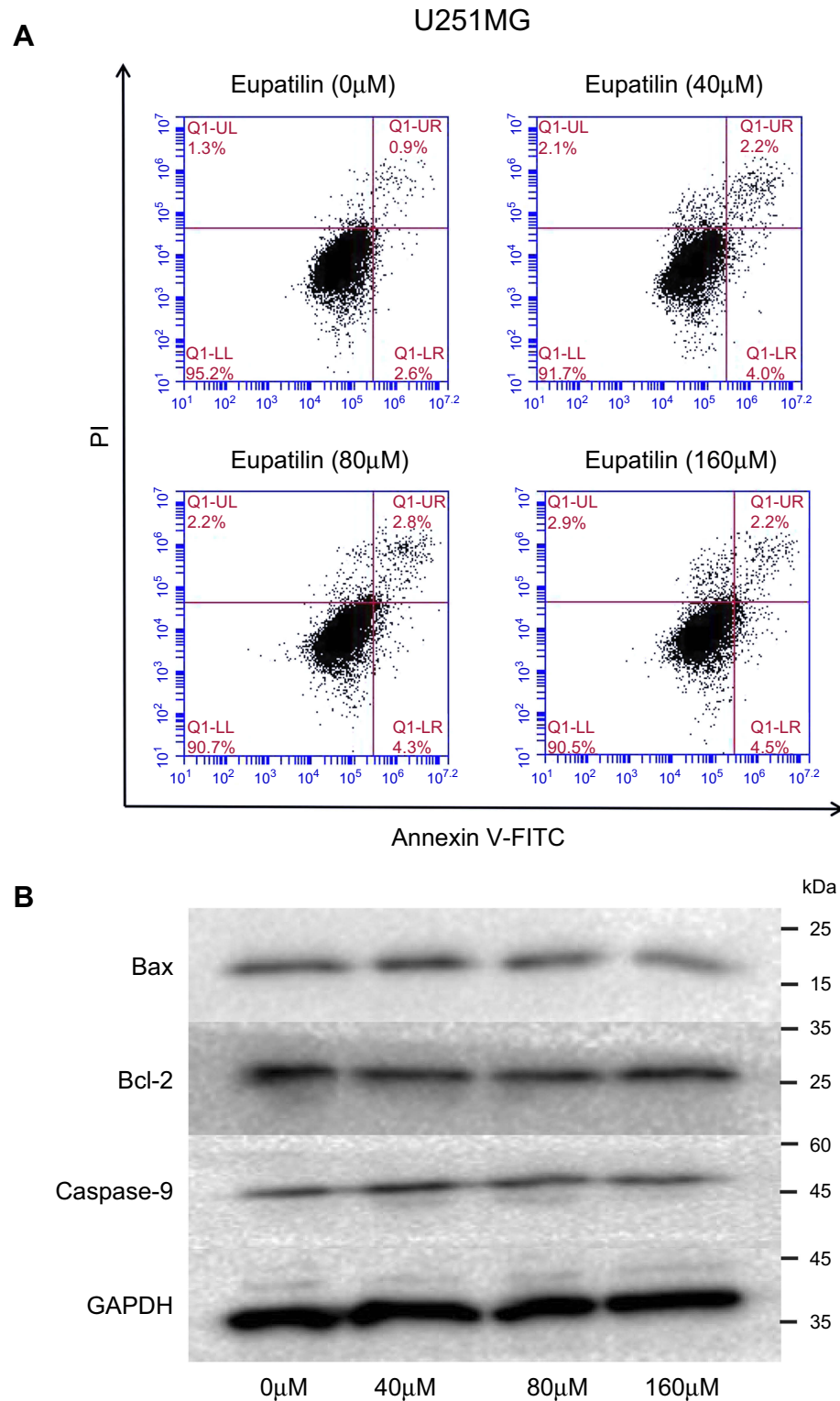
Supplementary material

A   U251MG

Figure S1 Effect of Eupatilin on apoptosis of glioma cells. (**A**) After treatment of each cell line with different concentrations(0, 40, 80, 160 **µM**) of eupatilin for 48 hrs, FITC Annexin V Apoptosis Detection Kit with PI kit was stained and detected by flow cytometry. (**B**) After treatment of each cell line with different concentrations(0, 40, 80, 160 µM) of eupatilin for 48 hrs, we harvested cells and detected apoptosis-related proteins by Western blot. The figure shows the result of U251MG.